M. F. Mecklenburg,[1] *C. O. Arah,*[2] *D. McNamara,*[2] *H. Hand,*[2] *and J. A. Joyce*[3]

Adhesive Fracture Testing

REFERENCE: Mecklenburg, M. F., Arah, C. O., McNamara, D., Hand, H., and Joyce, J. A., **"Adhesive Fracture Testing,"** *Fracture Mechanics: Twenty-First Symposium, ASTM STP 1074,* J. P. Gudas, J. A. Joyce, and E. M. Hackett, Eds., American Society for Testing and Materials, Philadelphia, 1990, pp. 307–321.

ABSTRACT: The need for lightweight materials for a variety of applications has resulted in the use of structural adhesives to bond prototype structures. Adhesives developed to accommodate the stringent requirements of these high-technology applications are usually deficient in one or two of three very crucial properties: strength, moisture resistance, and toughness. So far, advances in adhesive formulation that have ameliorated one of these deficiencies have generally adversely affected the others. Hence a considerable amount of effort is being expended in the search for strong, moisture resistant, and tough adhesives.

As adhesives become tougher and less brittle, evaluating their performance in terms of fracture parameters becomes more complicated. Linear elastic fracture mechanics (LEFM), which is widely used to characterize these materials, does not fully describe adhesive performance as more and more ductility or plastic deformation is introduced. In the study reported here, we introduce the energy separation method for characterizing the fracture resistance of adhesives and compare it with currently used elastic and plastic fracture parameters such as G and the J integral. Both neat and bonded ½ CT plan specimens were tested and compared in this work.

KEY WORDS: elastic-plastic fracture, structural adhesive, neat bonded fracture, fracture toughness, energy separation

During a research program to develop a strong, moisture-resistant, ambient-temperature-curing, structural adhesive, we found a consistent reduction in ductility (as measured by neat material tensile tests) as strength and moisture resistance improved. This effect was primarily due to the higher crosslink densities in the modified stock epoxy adhesives we were using. Our immediate concern, however, was the fracture resistance of the modified epoxies and how to reliably characterize it so that it could be related to joint performance (e.g., correlate modifications to adhesive chemistry with adhesive fracture parameters).

A review of the fracture characterization options for our anticipated tougher adhesives indicated that the most useful parameters would be the elastic energy released, the plastic energy dissipated, and the potential energy of the test specimen at any crack extension. Linear elastic fracture mechanics (LEFM), which is widely used to characterize these materials, would not be applicable as ductility or plastic deformation increased.

The J integral [*1*] was explored because of its application to nonlinear elastic material behavior. For the adhesive geometry of interest the HRR singularity field could not be expected, but the J integral parameter still generally provides a useful experimental parameter to evaluate the relative material toughness of materials falling outside the LEFM regime.

[1] Conservation Analytical Laboratory, The Smithsonian Institution, Washington, DC 20560.
[2] Martin Marietta Laboratories, Baltimore, MD 21227.
[3] Department of Mechanical Engineering, U.S. Naval Academy, Annapolis, MD 21402.

The J integral parameter was not fully satisfactory for this application, since it was found to be relatively insensitive to the overall failure mode of the adhesive bond. The J fracture parameter is, in effect, a single-value parameter combining elastic and plastic energy components of crack growth resistance. We needed a clearer distinction of these energies, however, because some types of polymer modification would have a large effect on elastic component while others would influence the plastic component. Ting and Cottington [*2*] gave clear indications of experimental procedures that might be useful, even though they primarily concentrated on the elastic energy component of adhesive fracture testing. The method we chose for characterization was an energy separation technique [*3*] that clearly distinguishes crack growth energies and employs a standard, single-specimen, unload compliance test procedure commonly used in J integral testing [*4*].

Computation Methods

Energy Separation Method

The area under the plot of a load versus load-line displacement record is the sum of all the energies—elastic, plastic, and potential—applied to a fracture test specimen during crack initiation and extension. The work, W, done by the external load, P, can be related to the internal energy, U, by

$$dW = dU_s + dU_e + dU_p \tag{1}$$

where

W = work done by external load,
U_s = stored elastic strain (potential) energy,
U_e = elastic energy released during crack extension, and
U_p = plastic energy dissipated during crack extension.

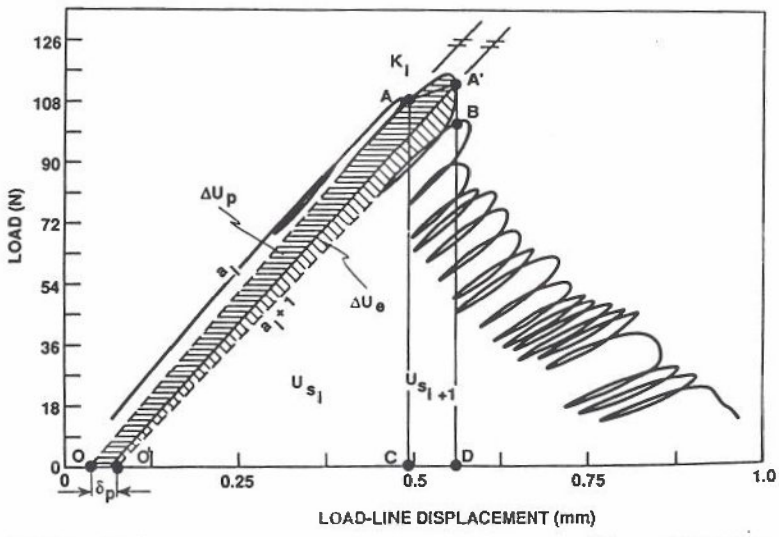

FIG. 1—*Partitioned load versus load-line displacement record for specimen M2A.*

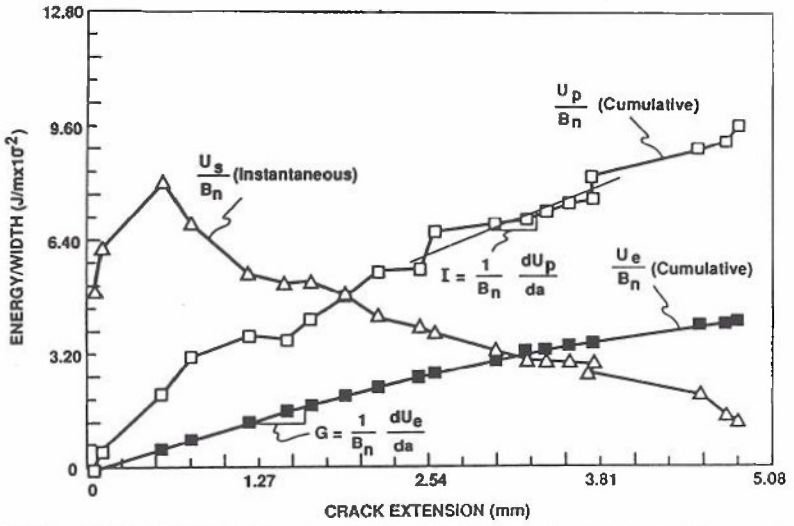

FIG. 2—*Cumulative energies released and stored versus crack extension for adhesive specimen M2A.*

These energies are depicted in Fig. 1, which illustrates an unload compliance, load versus load-line displacement record of a neat adhesive ½ CT plan specimen. Here the specimen is side-grooved 20% giving B = 6.35 mm (0.25 in.) and B_n = 5.08 mm (0.20 in.). In Fig. 1:

- Area $OAA'O' = U_p$
- Area $O'A'B' = U_e$
- Area $O'BD = U_s$ after crack extension (U_{si+1})
- Area $OAC = U_s$ prior to crack extension (U_{si})

The total resistance to a crack growth increment, da, is the sum of the plastic energy dissipated, dU_p, and the elastic energy released, dU_e. The total rate of energy release and dissipation with respect to crack growth can be expressed mathematically as

$$J_{ES} = G_{ES} + I = 1/B_n\, dU_e/da + 1/B_n\, dU_p/da \qquad (2)$$

where

J_{ES} = total energy release rate,
G_{ES} = elastic energy release rate,
I = plastic energy dissipation rate, and
B_n = net specimen width between side grooves.

Figure 2 shows the width normalized, cumulative sums of the plastic energies dissipated, and the elastic energies released and plotted with respect to the crack extension. As can be seen, G_{ES} is the slope of the cumulative released elastic energy normalized by the net width, and I is the slope of the cumulative dissipated plastic energy normalized by the net width. Also shown in Fig. 2 is the instantaneous value of the stored potential energy, U_s/B_n, at any crack extension. Neither of the curves is linear with respect to crack extension (i.e., their respective slopes are not constant and the values of G and I are not independent of crack

length). Nevertheless, by holding specimen size and initial crack length constant, the approach outlined above provides a clear method for comparing the specific effects of modifying the adhesive chemistry to the different aspects of fracture resistance.

The quantities G_{ES} and I are obtained from the test load, load-line displacement records and hence include the full specimen energy release and energy dissipation, respectively. Both quantities come in part from crack growth and in part from elastic energy released and plastic energy dissipated in the specimen well away from the crack tip region. The inability to separate the near and far components is a major drawback to any energy method. In this study, where all inelastic deformation is confined to the adhesive and in which the specimen size and geometry is not varied, it is felt that the energy method provides a useful measure of material toughness. Difficulties encountered with the application of J integral methods are discussed in the following section.

Figure 3 illustrates the crack length dependency with plots of G_{ES} and I against crack extension. After an initial jump both G_{ES} and I decrease with crack extension. To ensure reliable correlations during the adhesive study in the presence of this crack length dependency, all specimens were made identical in size and precracked to the same initial crack length. For comparison, a crack growth of 0.762 mm (0.030 in.) beyond the initial crack length was selected, since that interval generally coincides with the onset stable crack growth. This point is indicated by the vertical dashed line in Fig. 3.

Comparisons with J Integral

The usefulness of the energy separation method can be assessed by comparing it with the J integral method. In his original derivation of the J integral, Rice [*1*] was fairly explicit in relating J to body potential energy, whether the material behavior was linear or nonlinear. By assuming that elastic-plastic material behavior could be treated as nonlinear elastic material behavior in the absence of unloading, Rice, Paris, and Merkle [*5*] concluded that J for

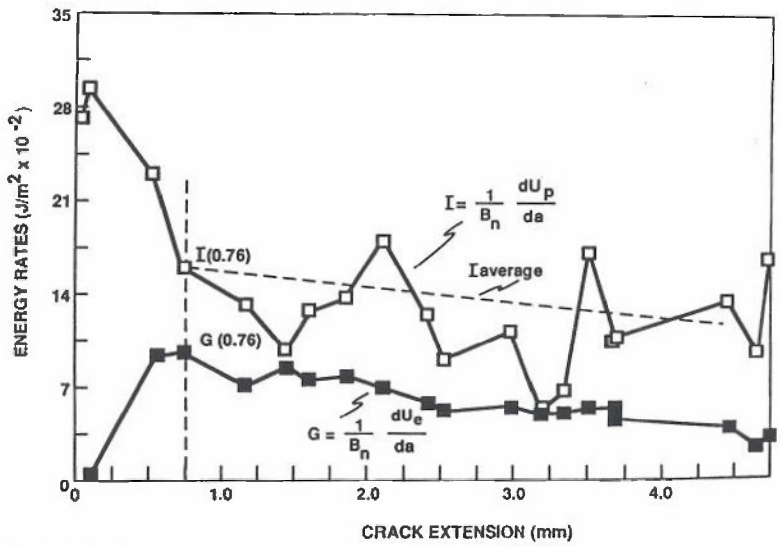

FIG. 3—*Elastic energy release rate and absolute plastic energy dissipation rate versus crack extension for specimen M2A.*

the deeply cracked bend bar could be expressed as

$$J = 2A/B_n b \tag{3}$$

where

A = total area under the load versus load-line displacement record,
b = remaining ligament of test specimen, and
B_n = net width of test specimen.

The coefficient 2 in Eq 3 was modified to account for the tensile component of stress present in the compact tension specimen and designated by η. In general, the current calculation of the J integral takes the form

$$J = \eta U/B_n b = J_{el} + J_{pl} = G_{ES} + J_{pl} = \eta U_s B_n d + \eta U_p/B_n b \tag{4}$$

where

J_{el} = elastic component of J,
J_{pl} = plastic component of J,
η = a coefficient related to the type of specimen,
U = total area under the load versus load-line displacement record, and
U_s, U_p, B_n, b, and G_{ES} are as defined previously.

In the specific case of calculating the elastic energy release rate, G is now taken to be

$$G_q = K_q^2(1 - \nu^2)/E \tag{5}$$

where K_q is the stress intensity factor as calculated from ASTM E 399.

Experimental work, described more fully below, showed that the elastic modulus of the aluminum could be used for bonded specimens in this conversion, while for neat specimens the adhesive elastic modulus was used as obtained from tensile tests of the adhesive material.

The applicability of the adherend elastic modulus for this calculation for the bonded specimens should be similarly verified if either the adherend or the adhesive is changed markedly.

We can now make some observations relating energy separation to the J integral by calculating G in several different ways and by comparing those values to the values obtained by the energy separation method. It may be seen from Eqs 2, 4, and 5 that

$$G = K_q^2/(1 - \nu^2)/E = 1/B_n\, dU_e/da = \eta U_s/B_n b \tag{6}$$

which apparently relates the stress intensity factor K_q, as calculated by ASTM E 399, to the instantaneous potential energy of the test specimen, U_s, and also to the elastic energy released, U_e. Figure 4 illustrates the results of evaluating G by the three expressions: from K_q, as determined from ASTM E 399; from energy separation using the increment of elastic energy release, $G_{ES} = 1/B_n\, dU_e/da$; and from energy separation, but using the instantaneous value of the potential energy, $G_{PE} = \eta\, U_s/B_n$, where $\eta = 2.3$. As can be seen, results of all three calculations compare favorably in spite of plastic deformation, suggesting that the method of partitioning the different energies is consistent with current theory. The last form of calculation (i.e., G_{PE}) permits G to be determined at the initiation of unstable crack growth.

The major drawback found in this work to the application of J to characterize the fracture toughness of the adhesive material and adhesively bonded specimens was the relative insen-

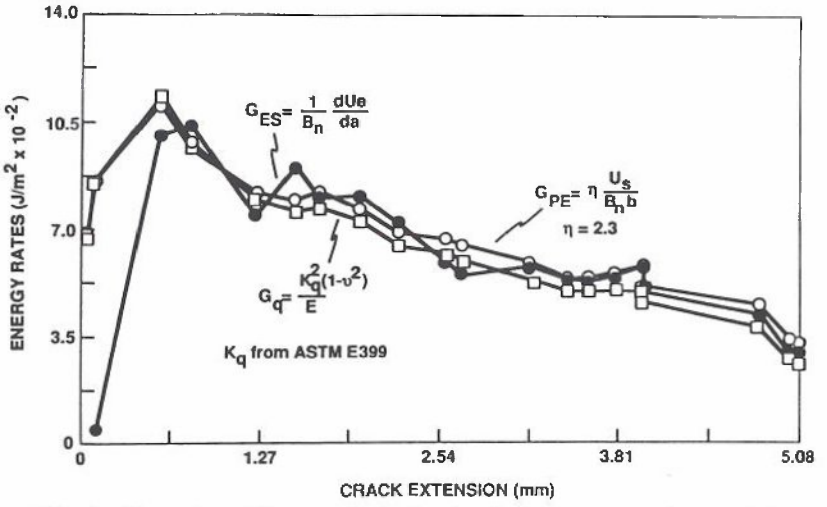

FIG. 4—*Comparison of three methods of evaluating G using neat adhesive M2A.*

sitivity of J to the demonstrated fracture behavior. Generally, for these tests, a tradeoff occurred between the elastic J component and the plastic J component, giving relatively small changes in J at crack initiation in spite of dramatically different specimen behaviors. Utilization of only the plastic J component was considered, but it appeared that the use of I, as given by Eq 2, gave a better measure of material toughness and was more sensitive to changes in adhesive chemistry and moisture content.

The J integral treats U_p (non-recoverable) as a component of the potential energy U_s (recoverable), whereas the energy separation method treats U_p as a post-crack extension quantity similar to U_e. As a consequence, I becomes a large value when U_p is divided by a small quantity, da, whereas J_{pl} is a relatively small quantity since U_p is divided by the total remaining ligament b. Hence the significance of U_p might be lost when it is combined to form the total quantity J. As we will show in our experimental results, G for our tests adhesives does not vary dramatically, while I can show substantial difference from one adhesive type to another.

Experimental Procedures

All specimens, either neat adhesive or bonded, were ½ CT plan with B = 6.36 mm (0.25 in.). Neat specimens were molded with a side groove to give B_n = 5.08 mm (0.20 in.), while bonded specimens were ungrooved. The dimensions of the specimens are presented in Fig. 5. In both cases blunt notches were fabricated to a depth of about 10.5 mm and subsequently extended by pressing in a razor blade to produce a sharp starter crack of about 12.9 mm total depth.

The clip gage load-line attachment points were made integral to the specimen. The bulk specimens were cast in aluminum molds coated with release agents. Adherends for the bonded specimens were machined from aluminum and bonded in alignment jigs to provide a bondline thickness of about 0.254 mm (10 mils).

Surface preparation for all adhesive bonding in this program was done using Boeing Corporation's phosphoric-acid-anodization (PAA) process. This process has gained wide acceptance as the treatment which provides the most durable and reliable bonding surface for

aluminum. By selecting this process, we ensured that we were testing the properties of the adhesive materials, unclouded by uncertainties in adhesive-metal bonding. In addition, the PAA process is not very difficult to implement and is routinely used for large-scale airframe components.

The PAA process consists of the following steps:

1. Degreasing/surface cleaning in an alkaline soap bath.
2. Immersion rinse in distilled water.
3. Deoxidizing in an acid solution (we used the Forest Products Laboratory aluminum etch: 17 vol% concentrated sulfuric acid and 60 g/L sodium dichromate at 66°C (150°F) for 15 min).
4. Immersion rinse in distilled water.
5. Anodizing in 10 wt% phosphoric acid solution at 10 V (specimen attached to the positive terminal) for 20 min at room temperature.
6. Immersion rinse in distilled water.
7. Air dry.

The resultant surface exhibits water-break-free behavior during rinsing and a blue-green iridescence when viewed at grazing incidence.

The oxide surface produced by the PAA process on aluminum consists of a "forest" of extremely fine whiskers (roughly 100 Å across) that can mechanically interlock with the epoxy polymers, producing a very rugged bond. The phosphorous ions in the solution, which are incorporated into the oxide during the anodizing, prevent moisture from attacking the oxide film. Thus bonds to PAA surfaces are also more durable than those surfaces treated by other means.

The crack length, a, was determined using the elastic compliance method and the empirical equations as provided in ASTM E 1152. In general, we found that the crack length could be more accurately obtained if the unloading was at least 20% of the current maximum load. Measured crack lengths agreed well with those calculated by the empirical equation for both the neat and bonded compact specimens. The results of this comparison are presented in Fig. 6.

The modulus of elasticity, E, was determined in a tensile test on neat specimens, and was used for the crack length determination and the calculation of K_q. For the bonded specimens, we used the modulus of the aluminum.

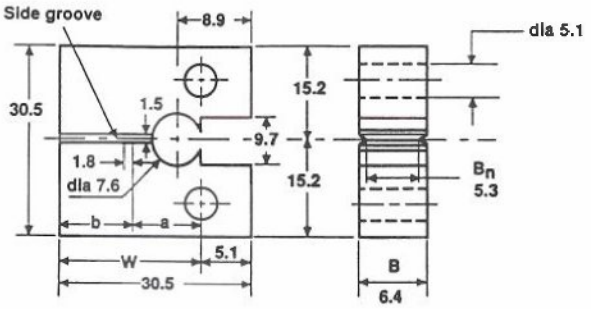

FIG. 5—*Compact tension ½ specimen dimensions.*

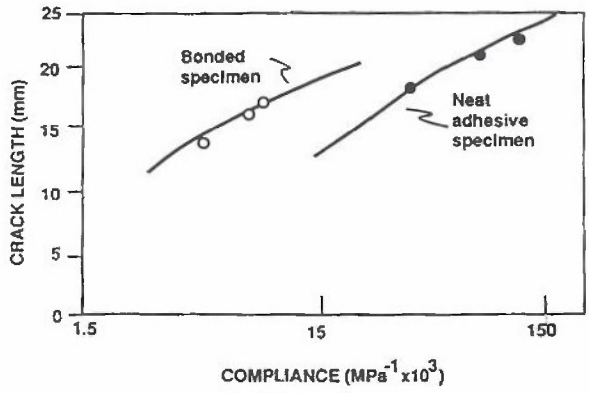

FIG. 6—*Comparison of calculated* (solid line) *and experimental* (circles) *plot of crack length as a function of compliance.*

Results and Discussion

Neat Adhesives

Test results of the different neat adhesives varied widely, displaying considerable differences in load magnitudes at crack initiation as well as plastic deformation. Three examples of typical neat adhesive, unloading compliance, load versus load-line displacement records are shown in Figs. 7*a–c*, which show respectively: (*a*) material that experienced a brittle,

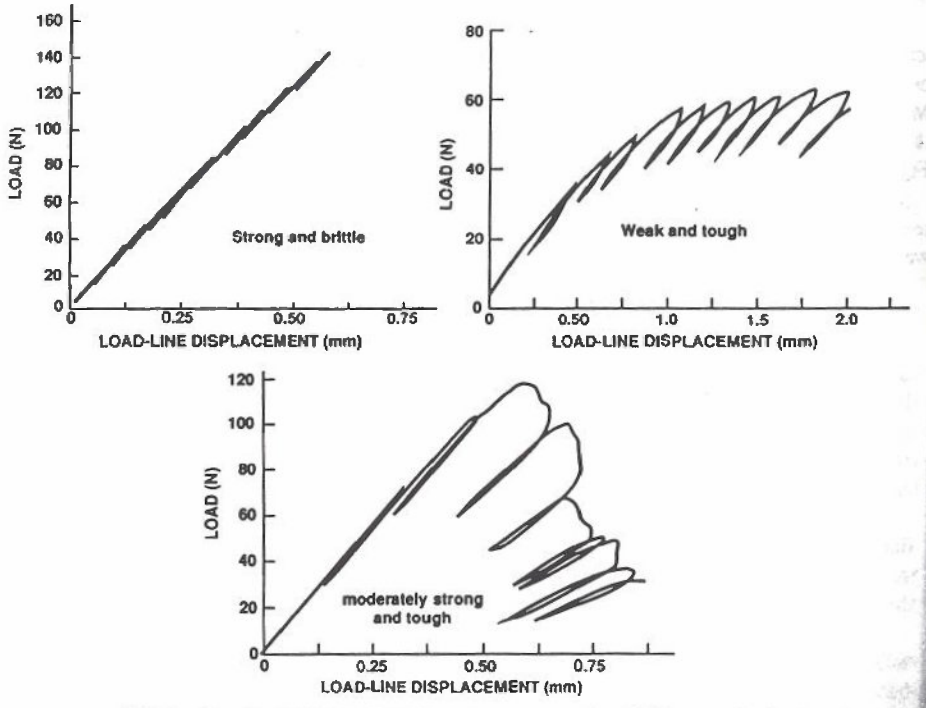

FIG. 7—*Load versus load-line displacement records of different adhesives.*

unstable failure at about 156 N (35 lb) but was quite moisture resistant; (*b*) very tough but weakly adhesive behavior with little resistance to moisture; and (*c*) a moderately tough and strong adhesive with some moisture resistance. Moisture resistance was determined separately in adverse environments using stress relaxation tensile tests on bulk specimens [*6*].

Some typical results for G_{ES} and I are shown in Table 1 for fracture tests on neat adhesive compact tension specimens; J is included for comparison. All values listed (average of three tests) were taken at a crack extension of 0.762 mm (0.03 in.). G_{ES} and I are calculated by the energy separation method except in the case of brittle fracture, where G was calculated from Eq 5. J was calculated as defined by ASTM E 1152. Within a single specimen, G_{ES} and G_q maintained moderately constant decreasing values over the crack extension examined and had a standard deviation of less than or equal to 20% from specimen to specimen of the same type of adhesive. I values were more variable both within the same specimen and from specimen to specimen. Of all variables influencing the test results, crack extension was the most difficult to measure reliably. Crack length measurements improved with deeper unloadings, better determination of the values of E, and more accurate load-line displacement measurements.

The wide variations in I from adhesive to adhesive shown in Table 1 had nearly no correlation to the elongation to failure data as measured in a tensile test. Table 2 shows typical results of the neat specimen tensile testing. Of particular interest are Adhesives 14 and 96, which show moderate tensile elongations but completely brittle fracture.

TABLE 1—*Fracture toughness results on neat adhesive specimen (average of at least three tests).*

	G_{ES}		I		J		Peak Load	
Adhesive	J/m^2	(in.-lb/in.^{2})	J/m^2	(in.-lb/in.^{2})	J/m^2	(in.-lb/in.^{2})	N	(lb)
1	650	(3.7)	735	(4.2)	825	(4.7)	142	(32)
3	1450	(8.3)	1020	(5.8)	1910	(10.9)	151	(34)
5	615	(3.5)	3270	(18.7)	1540	(8.8)	62	(14)
100	1820	(10.4)	4850	(27.7)	3150	(18.0)	258	(58)
14	1930[a]	(11.0)	0	0	1930[a]	(11.0)	160	(36)
17	630[a]	(3.6)	0	0	630[a]	(3.6)	124	(28)
96	1260[a]	(7.2)	0	0	1260[a]	(7.2)	138	(31)
98	1380[a]	(7.9)	0	0	1380[a]	(7.9)	156	(35)

[a] Specimen showed totally brittle behavior; $G_{ES} = G_{PE} = J$.

TABLE 2—*Tensile test values for neat adhesives.*

	Ultimate Tensile Strength		Modulus		
Adhesive	MPa	(psi)	MPa	(ksi)	Elongation, %
1	61.8	(8960)	2830	(410)	2.8
3	52.8	(7650)	2280	(330)	5.4
5	14.9	(2160)	760	(110)	10.6
100	57.5	(8340)	2830	(410)	2.8
14[a]	60.9	(8830)	2280	(330)	5.4
96[a]	73.9	(10710)	2690	(390)	6.3
98[a]	61.8	(9520)	2280	(330)	4.9

[a] Denotes model adhesives developed for this program. The other adhesives are commercially available room-temperature-cure systems.

Bonded Specimens

Fracture characterization data indicated that, in general, bonded specimens were more stable and demonstrated greater load capacities than neat specimens. Figure 8 shows load versus load-line displacement plots of ½T CT neat and bonded test specimens identical in size and type for the same adhesive. The stiffer bonded specimen exhibits considerably less load-line displacement than the neat specimen and withstands over three times the load at crack initiation.

Typically, bonded specimens remained stable throughout the test procedure, while neat specimens were unstable beyond the initiation of crack extension. Comparing the adhesive toughness in terms of J and G generated the appearance of similar values, an appearance felt to be very misleading in terms of the expected performance in the intended application where strength and stable behavior were desired. Comparison of the adhesive toughnesses based only on I at initiation shows that, on this basis, the bonded specimens are tougher and should be more stable than the neat specimens. Typical results for the bonded specimens are presented in Table 3. For the case where brittle behavior was observed G was taken as G_{PE} and was identical to J. For Adhesives 5 and 14 (Fig. 9) G_{ES} was found to be greater than G_{PE} or J at initiation, while for Adhesives 11, 3, 100, and 96 the reverse was true. In all cases it was I that related directly to the desired application properties of high bond strength and stable crack growth.

The values of G_{ES} (or G_{PE}) for the bonded specimens are similar to, but slightly lower than, those of the neat specimens, and bondline failure was always cohesive in these cases. When the bondline failed at the adhesive-adherend interface, the values of G_{ES} dropped substantially; I for the bonded specimens was routinely higher, consistent with their more stable crack growth.

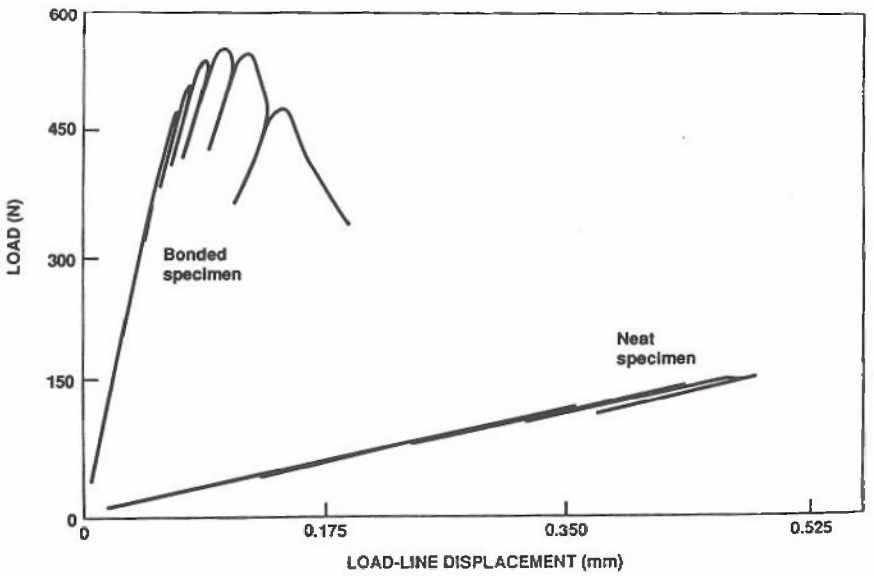

FIG. 8—*Comparison of the load versus load-line displacement records for bonded and neat adhesive specimens.*

TABLE 3—*Fracture toughness results for bonded specimens (average of at least three tests).*

	G_{ES}		I		J		Peak Load	
Adhesive	J/m²	(in.-lb/in.²)	J/m²	(in.-lb/in.²)	J/m²	(in.-lb/in.²)	N	(lb)
1	735	(4.2)	3470	(19.8)	790	(4.5)	663	(149)
3	860	(4.9)	2170	(12.4)	1240	(7.1)	614	(138)
5	610	(3.5)	2080	(11.9)	525	(3.0)	334	(75)
100	1450	(8.2)	7000	(40.0)	1930	(11.0)	952	(214)
14	665	(3.8)	210	(1.2)	370	(2.1)	583	(131)
96	700	(4.0)	470	(2.7)	719	(4.1)	494	(111)
98	1380[a]	(7.9)	0	(0)	1380[a]	(7.9)	494	(111)

[a] Specimen showed totally brittle behavior; $G_{ES} = G_{PE} = J$.

Adherend Stiffness Effects

The most probable explanation for the differences in behavior is the substantial difference in the stiffness of the two types of specimens. The aluminum adherends, which are quite stiff relative to the bondline adhesive, can provide considerable mechanical constraints on the adhesive as well as allow for more uniform rotation of the specimen during loading. More uniform rotation of the adherend produces more uniform distribution of the entire bondline normal stresses, which reduces the concentration of stress at the crack tip and allows the specimen to sustain a higher load. On the other hand, the neat specimen is more flexible as demonstrated by the greater load-line displacement and tends to "peel" apart, which concentrates stresses nearer the crack tip and allows a smaller load to initiate crack growth. These effects are illustrated in Figs. 10 and 11. Figure 10 presents the elastic plane-strain finite element bondline stress analysis for the aluminum-bonded specimen. The specimen used as the model was bonded with Adhesive 100, which has a maximum load capacity of 952 N (214 lb) and a modulus of 2830 MPa (410 ksi); the modulus used for the aluminum adherend was 73.1 GPa (10.6 × 10^3 ksi). The bondline used in the model was 0.381 mm (0.015 in.) thick. The stress distribution along the bondline over the remaining ligament is quite uniform. For the stress distribution to be this uniform, the aluminum adherends must be uniformly rotating during the loading of the test specimen. On the other hand, the neat specimen stress analysis (Fig. 11) presents a stress distribution that is quite non-linear, with a

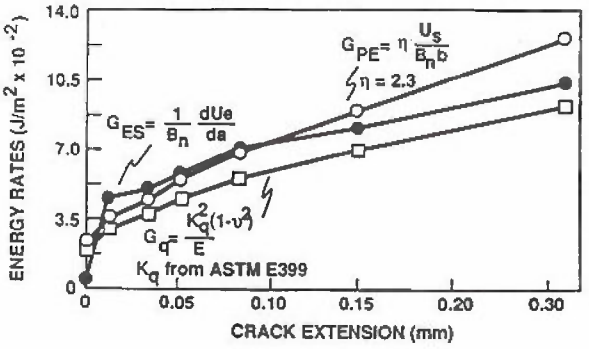

FIG. 9—*Comparison of three methods of evaluating G using bonded adhesive #14.*

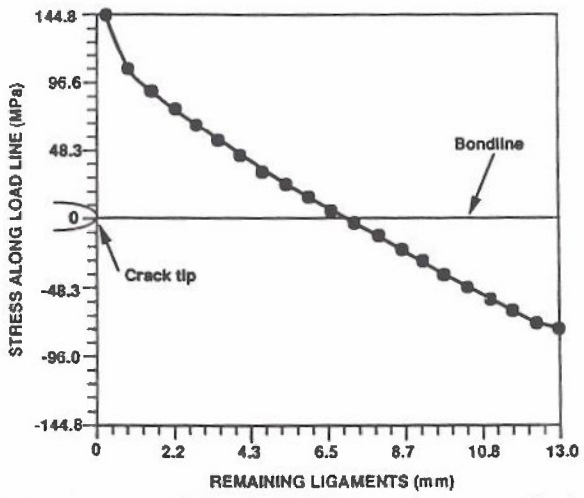

FIG. 10—*Finite element analysis of a bonded ½ CT specimen showing elastic stress distribution.*

severe concentration near the crack tip. The same model geometry was used for both finite element analyses (Figs. 10 and 11), but a value of 2830 MPa (410 ksi) was used as the modulus of the entire neat specimen and the maximum load applied was 258 N (58 lb). The more flexible neat specimen is seen to "peel" apart, leading to progressive crack growth and development of a load-carrying capacity below the full potential of the bondline.

Conclusions

The fracture performance of both neat and bonded adhesives can be effectively compared on a very small compact tension specimen using the unload compliance procedure. Using this approach we can make a better evaluation of changes in adhesive chemistry.

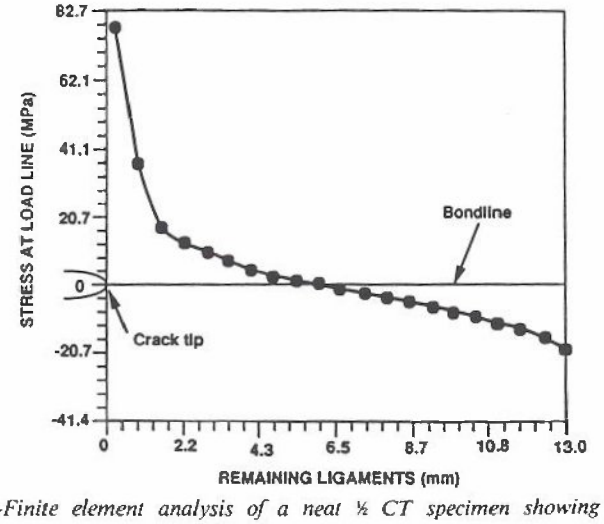

FIG. 11—*Finite element analysis of a neat ½ CT specimen showing elastic stress distribution.*

The energy separation method described here allows G_{ES} to be measured directly from the test record using either the increment of released energy, dU_e, or the instantaneous value of the potential energy, U_s. Either measurement correlates well to current theory.

The parameter I, as derived with the energy separation method, provides a distinct and sensitive measurement of the plastic component of fracture resistance.

Since all the parameters discussed in this study are dependent on the crack length, care must be used to maintain consistent specimen size and geometry including the initial crack length.

Compared with neat adhesive specimens, bonded specimens sustained more than three times the load at crack initiation and consistently exhibited greater crack growth stability, even when the neat specimens showed brittle behavior.

The calculated values of J suggest that the neat adhesive specimens resist crack growth better than the bonded specimens, contrary to experimental observations. This discrepancy is primarily due to the under-representation of the plastic energy component in the computation of J. Results of the energy separation technique, however, clearly show the superiority of the bonded specimens in resisting crack growth, as reflected in the values of I.

Acknowledgments

We gratefully acknowledge financial support for Martin Marietta from the U.S. Army Troop Support Command's Belvoir Research, Development and Engineering Center under Contract DAAK-70-86-0084.

References

[1] Rice, J. R., "A Path Independent Integral and the Approximate Analysis of Strain Concentration by Notches and Cracks," *Journal of Applied Mechanics*, Vol. 35, 1968, p. 379.

[2] Ting, R. Y. and Cottington, R. L., "Comparison of Laboratory Techniques for Evaluating the Fracture Toughness of Glassy Polymers," *Journal of Applied Polymeric Science*, Vol. 25, 1980, p. 1815.

[3] Mecklenburg, M. F., Joyce, J., and Albrecht, P., "Separation of Energies in Elastic-Plastic Fracture," in *Non-Linear Fracture Mechanics: Volume II—Elastic-Plastic Fracture, ASTM STP 995*, American Society for Testing and Materials, Philadelphia, 1989, p. 594.

[4] Joyce, J. A. and Gudas, J. P. in *Elastic-Plastic Fracture, ASTM STP 668*, American Society for Testing and Materials, Philadelphia, 1979, p. 451.

[5] Rice, J. R., Paris, P. C., and Merkle, J. G., in *Progress in Flaw Growth and Fracture Toughness Testing, ASTM STP 536*, American Society for Testing and Materials, Philadelphia, 1974.

[6] Albrecht, P., Mecklenburg, M. F., Wang, J., and Hong, W., "Effect of Environment on Mechanical Properties of Adhesives," Final Report, Office of Research, Development, and Technology, Federal Highway Administration, Contract DTFH-61-84C-00027, Feb. 1987.

DISCUSSION

C. E. Turner[1] *(written discussion)*—This writer entirely supports the authors' use of dU_{pl}/Bda as a meaningful measure of toughness, implying that toughness is a plastic work dissipation rate associated with the separation process. The writer will not, however, use the symbol I for that term, since he has previously used it (e.g., [*1*] and at more length [*2*]) for "the other side of" the instability equation, namely, the "elastic energy release rate in the presence

[1] Mechanical Engineering Department, Imperial College, London, England.

of plasticity". Thus, by mischance, ductile instability expressed as "energy relcase rate (including compliance)" = "work absorption rate" would become (Turner)/(geometric factor) = (Mecklenburg et al.)! Moreover, the authors' Fig. 1, showing elastic and plastic energy rates, is misleadingly similar to that used by the writer to define I (Turner). The differences are, however, most important.

It is not clear whether in Fig. 1 the line $O'A'$ is parallel to OA. If it is, there would seem to be no crack growth during the essentially constant load behavior, AA'. If the lines are not parallel, implying that there is growth, then surely there is an elastic component within $OAA'O'$? The analysis assigns the plastic work $OAA'O'$ to growth during the whole period $AA'B$. Strictly, since point B is marked on the next reloading loop, these remarks refer to a point, say B', just above B as the load falls from A'. The combination into one analysis of what appears to be a period of either no growth or stable growth (during AA', according to whether or not the lines are parallel) with a period of apparently unstable growth (during $A'B'$ where the event is at fixed displacement) seems to merit further explanation.

The comparison made between I (Mecklenburg et al.) and J is moreovcr rather misleading in that dJ/da is not mentioned. Yet I (Mecklenburg) relates to dJ/da rather than J. The precise relationship depends on the definition of J after growth, but the leading term in any definition follows from the first term in the differentiation of $J = \eta U/Bb$ as $dJ_0/da = \eta(dU/da)/Bb$ (here written as dJ_0 to distinguish it from the many other definitions in use). Thus I (Mecklenburg) = $(b/\eta)(dJ_0/da)$, and its decreasing valuc (shown, for example, in Figs. 3 and 4) would be reflected in the decreasing slope of the conventional J-R curve.

The point at issue appears to be does "toughness" imply to the user a normalized work, as in the evaluation of the conventional J and J-R curve formulae quoted above, or a work rate with respect to crack growth, as in the original LEFM usage and as dJ/da or I (Mecklenburg) would measure it? The emphasis in that question, as discussed in the writer's own (jointly authored) paper presented to this symposium, is not whether work or internal energy should be used, relevant though that is [*3*], but rather whether the quantity or its crack rate derivative, d/da, is the factor of interest. The question arises because prior to initiation both terms change in proportion so that one encompasses the other. That is also true for growth in LEFM plane stress, whereas in EPFM *after crack growth* work increases whilst work rate decreases. This was illustrated most clearly in a paper written by some of the same authors [*4*], which case was discussed at some length in the writer's presentation to the symposium. An answer can hardly be drawn here if 20 years of research have not yet produced it, although the writer believes that most would agree that prior to initiation any of the terms will serve as a measure of crack tip severity because work, work rate, and the HRR (including K for LEFM) crack intensity field can all be related, whereas after initiation it is the work rate that controls instability. In that case both terms are required separately since they have different numerical trends and different physical significance. What is lacking is a clear definition and agreed upon usage of two separate words, one of which will be continuous in meaning with LEFM. Since "toughness" there undeniably means "work rate", the implication is that that designation should be retained for dJ_0/da or I (Mecklenburg), subject to whether the geometric term η/b is included or not. A separate word or expression other than "toughness", such as "tearing resistance", should come then into use for J and J-R curve properties based on normalized work. Of course, the definition of η ensures that *up to initiation* the numerical value of the "tearing resistance" from $J = \eta A/Bb$ is the same as the "toughness" from $J = -dP/Bda$ (where A is area under the load-displacement diagram and P is potential energy with the usual reservations on plasticity with no unloading), but after initiation the two terms would differ. Both rise in contained yield but diverge rapidly as full plasticity is reached, "tearing toughness" (from work) continuing to rise but "toughness" (from work rate) falling with growth.

In the writer's opinion this lack of an agreed upon terminology has led to the loose usage of the word "toughness" outside a strict LEFM connotation and has caused much confusion in the study of fracture in the EPFM regime.

Discussion References

[1] Turner, C. E. in *Fracture Mechanics (Eleventh Conference), ASTM STP 677*, 1979, pp. 614–628.
[2] *Post-Yield Fracture Mechanics*, D. G. H. Latzko et al., Elsevier Applied Science, 2nd ed., 1984, Chap. 2.
[3] Etemad, M. R. and Turner, C. E., *International Journal of Pressure Vessels and Piping*, 1985, pp. 81–88.
[4] Mecklenburg, M. F., Joyce, J. A., and Albrecht, P., "Separation of Energies in Elastic-Plastic Fracture," *Non-Linear Fracture Mechanics: Volume II—Elastic-Plastic Fracture, ASTM STP 995*, American Society for Testing and Materials, Philadelphia, 1989, pp. 594–612.

M. F. Mecklenburg et al. (authors' closure)—The authors thank Professor Turner for his comments. Lines OA and $O'A'$ are intended to be parallel, as is clearly stated in Ref *3*. Our use of the geometric construction in Fig. 1 is in no way an attempt to describe the sequence of events leading to elastic and plastic energy releases. This construction was simply a way to illustrate the total difference between the released elastic energy, U_e, and the dissipated plastic energy, U_p.

We use the letter I to mean the plastic energy dissipation rate, as shown in Eq 2; it is more fully described in Ref *3*.

FRACTURE MECHANICS

Twenty-First Symposium

Gudas / Joyce / Hackett

Editors

ASTM STP 1074

ASTM Publication Code Number (PCN): 04-010740-30
ISBN: 0-8031-1299-8
ISSN: 1040-3094

NOTE

The Society is not responsible, as a body,
for the statements and opinions
advanced in this publication.

Peer Review Policy

Each paper published in this volume was evaluated by three peer reviewers. The authors addressed all of the reviewers' comments to the satisfaction of both the technical editor(s) and the ASTM Committee on Publications.

The quality of the papers in this publication reflects not only the obvious efforts of the authors and the technical editor(s), but also the work of these peer reviewers. The ASTM Committee on Publications acknowledges with appreciation their dedication and contribution of time and effort on behalf of ASTM.

Printed in Baltimore, Md.
August 1990

Foreword

The ASTM Twenty-First National Symposium on Fracture Mechanics was held in Annapolis, Maryland, on 28–30 June 1988. Its sponsor was Committee E-24 on Fracture Testing.

The co-chairmen for this symposium were John P. Gudas, David Taylor Research Center; James A. Joyce, United States Naval Academy; and Edwin M. Hackett, David Taylor Research Center. They have also served as editors of this volume.